

# A Spiking Neural Network Model Mimicking the Olfactory Cortex for Handwritten Digit Recognition

Ben-Zheng Li, *Member, IEEE*, Sio Hang Pun, *Member, IEEE*, Wan Feng, *Member, IEEE*, Mang I Vai, *Senior Member, IEEE*, Achim Klug, and Tim C. Lei, *Member, IEEE*

**Abstract**—The mammalian olfactory system uses odor-specified temporal codes to represent the quality and the quantity of different odors. In order to better understand this coding strategy, a biologically plausible spiking neural network (SNN) was built and evaluated. In this study, MNIST images of handwritten digits were used to mimic the two-dimensional representation of odor information by the glomeruli in the olfactory bulb. The images were used to train the SNN based on the spike-timing-dependent plasticity (STDP) unsupervised learning rule. The SNN model was implemented by Izhikevich neurons to represent both the pyramidal neurons and the GABAergic interneurons in the piriform cortex. The recognition accuracy of the SNN model was evaluated to gain insights for the temporal coding scheme in the olfactory system. The results suggested that the SNN model can effectively encode 2D neural representations with temporal codes and achieved discrimination accuracies close to animal behavioral performances in odor discrimination tasks.

## I. INTRODUCTION

In the central nervous system, odor discrimination plays an essential role in survival and danger avoidance for animals in their natural habitats. In addition, the olfactory sensory system exhibits similar anatomical structures across different animal species suggesting that a common neural coding scheme has been preserved throughout evolution [1]. From a signal processing perspective, odor recognition can be considered as a pattern recognition process. Olfactory sensory neurons expressing different odorant receptors are sensitive to different chemical compositions of odorants, and these sensory neurons are scattered across the olfactory epithelium to maximize odor sensitivity. The axons of olfactory sensory neurons expressing the same odorant receptors converge to form glomeruli in the olfactory bulb. Therefore, each glomerulus encodes a specific chemical component, and these glomeruli are organized into a two-dimensional structure in the olfactory bulb [2]. When an odor is comprised of several chemical components stimulating the olfactory sensory neurons, the olfactory sensory neurons generate a unique neural coding pattern in the olfactory bulb. The downstream neural regions, including the mitral and tuft cells in the olfactory bulb and the olfactory cortex, interpret this encoded signal to determine odor qualities and quantities.

\* Research supported by the Science and Technology Development Fund of Macau (FDCT) under Grants 093/2015/A3, 088/2016/A2 and the University of Macau under Grants MYRG2014-00010-AMSV, MYRG2015-00178-AMSV, MYRG2016-00157-AMSV, MYRG2018-00146-AMSV, MYRG2015-00178-AMSV & MYRG2016-00157-AMSV.

Ben-Zheng Li is with the State Key Laboratory of Analog and Mixed-Signal VLSI, University of Macau, Macau, China and with the Department of Physiology and Biophysics, University of Colorado Anschutz Medical Campus, Aurora, CO 80045 USA.

Sio Hang Pun is with the State Key Laboratory of Analog and Mixed-Signal VLSI, University of Macau, Macau, China

The odor-evoked response can further be used by the brain to integrate with other sensory signals, such as visual and auditory information, at the higher cortical regions to determine for a behavioral response.

Spiking Neural Networks (SNNs) use artificial neural spikes to encode information for signal processing. Since the brain uses action potentials (biological neural spikes) for data processing, SNN is naturally a closer modeling system to mimic neuronal activities and the signal processing circuits in the brain, as compared to conventional Artificial Neural Networks (ANN). SNNs have recently been demonstrated to exhibit powerful computational capabilities and were applied to pattern recognition applications with successful outcomes [3]. Therefore, in this paper, we attempt to use SNN to model the olfactory sensory system and uses this model system to perform pattern discrimination tasks. The MNIST dataset is a collection of 2D images of handwritten digits. Since the olfactory information is also encoded in a semi-2D structure in the olfactory bulb, the MNIST dataset can then be loosely used to test our olfactory SNN model whether our SNN olfactory model can successfully separate these handwritten digits. Although this attempt was not ideal, the MNIST dataset may still lead to better understand of the coding principle for the olfactory sensory system and also promote the use of SNN in other pattern recognition applications.

Recent modeling attempts of the olfactory system were largely done by using ANN where spiking odor information were translated into byte words for classification. Despite these ANN olfactory models can be robust in classifying odor-evoked neural activities [4], [5], byte words, however, are foreign to a biological brain where action potentials (spikes) are used for information processing. SNNs, in contrast, closely mimic a biological brain in which temporal spiking activities are directly analyzed. In this study, we attempt to model the olfactory cortex directly using SNN, combining with the spike-timing-dependent plasticity (STDP) unsupervised learning rule, to understand how the olfactory system can use temporal spikes to differentiate 2D coding patterns. Handwritten digits [6] from the MNIST dataset was used and the pixel intensities were encoded by stochastically firing

Wan Feng is with the Department of Electrical and Computer Engineering, Faculty of Science, University of Macau, Macau, China

Mang I Vai is with the State Key Laboratory of Analog and Mixed-Signal VLSI, and with the Department of Electrical and Computer Engineering, Faculty of Science, University of Macau, Macau, China

Achim Klug is with the Department of Physiology and Biophysics, University of Colorado Anschutz Medical Campus, Aurora, CO 80045 USA.

Tim C. Lei (corresponding author) is with the Department of Electrical Engineering, University of Colorado Denver, Denver, CO 80204 USA. (e-mail: tim.lei@ucdenver.edu)

neural spike trains. The spike trains were then inputted to the SNN olfactory cortical model for training and discrimination. Discrimination accuracies were estimated to help guide future improvements of the SNN model.

## II. METHODS

### A. Neuron and Synapse Models

All spiking neurons used in the SNN model were implemented using Izhikevich neurons. Izhikevich neurons can provide a rich variation of neural firing patterns, similar to the Hodgkin-Huxley neurons, but with a much higher computational efficiency [7]. Izhikevich neurons use two 1<sup>st</sup>-order ordinary differential equations to calculate spiking activities [7],

$$\begin{aligned} v' &= 0.04v^2 + 5v + 140 - u + I_{\text{syn}} \\ u' &= a(bv - u) \end{aligned}$$

where  $v$  is the membrane potential of the spiking neuron,  $u$  is the membrane recovery variable, and  $I_{\text{syn}}$  is the synaptic current. A neural spike is elicited when  $v > V_{\text{peak}}$ , and  $u$  and  $v$  are reset based on the following after-spike resetting conditions,

$$\text{when } v > V_{\text{peak}}: \begin{cases} v \leftarrow c \\ u \leftarrow u + d \end{cases}$$

The  $a$ ,  $b$ ,  $c$ ,  $d$  parameters specify the recovery rates for different types of neurons. For the SNN model in this study, two settings were used to simulate regular spiking neurons with  $(a, b, c, d) = (0.02, 0.2, -65, 8)$  and fast-spiking neurons with  $(a, b, c, d) = (0.1, 0.2, -65, 2)$  [7].

A conductance-based synapse model was used to simulate the synaptic current  $I_{\text{syn}}$ . The synaptic current  $I_{\text{syn}}$  is expressed by the following equations,

$$\begin{aligned} I_{\text{syn}} &= g_e(E_e - v) + g_i(E_i - v) \\ \tau_e g_e' &= -g_e \\ \tau_i g_i' &= -g_i \end{aligned}$$

where  $g_e$  and  $g_i$  are the electrical conductances,  $E_e$  and  $E_i$  are the reversal potentials, and  $\tau_e$  and  $\tau_i$  are the time constants, for the excitatory and the inhibitory synapses respectively.

A synapse between the pre-synaptic and the post-synaptic pyramidal neurons was associated with a synaptic weight  $w$  for signal conductance. Spike-timing-dependent plasticity (STDP) unsupervised learning rule was then used to modulate this synaptic weight  $w$ . STDP, due to causality, strengthens the synaptic weight when a post-synaptic neuron fires right after the pre-synaptic neuron, but weakens the synaptic weight when the opposite firing sequence occurs. For computational efficiency, STDP was implemented using synaptic traces [8].

### B. Network Architecture and Parameters

The architecture of the SNN model was to mimic the primary olfactory cortex, also known as the piriform cortex. The primary olfactory cortex is a three-layered cortical structure consisting of glutamatergic excitatory pyramidal neurons and GABAergic inhibitory interneurons [1]. Anatomically, the lateral olfactory tract (LOT) projects the odor-evoked neural activities from the olfactory bulb onto the

layer 1 of the anterior piriform cortex, where both the inhibitory feedforward interneurons and the pyramidal excitatory neurons receive neural information from the LOT outputs [1], [9]. The pyramidal neurons located in the layer 2/3 are connected to another set of pyramidal neurons via the inhibitory feedback neurons which reside in the layer 3 [5], [9].

The SNN implemented, as shown in Fig. 1, was a four-layered network consisting of an input layer, i.e. LOT, and three other layers – the L2/3 pyramidal neuron layer, the L1 feedforward interneuron layer, and the L3 feedback interneuron layer. The input layer behaved similar to LOT, projecting the encoded sensory information to both the L2/3 pyramidal neuron layer and the L1 feedforward interneuron layer. The inhibitory neurons in the L1 feedforward interneuron layer were connected to the L2/3 pyramidal neurons to allow feedforward inhibition which limited the amount of signal integration for the pyramidal neurons in the early phases of bursting [9]. The L3 feedback interneurons received neural spikes from a subset of pyramidal neurons at L2/3 through excitatory synapses, and then fed their inhibitory outputs back to another random subset of pyramidal neurons at L2/3, resulting in lateral inhibitions for the neurons in the layer.

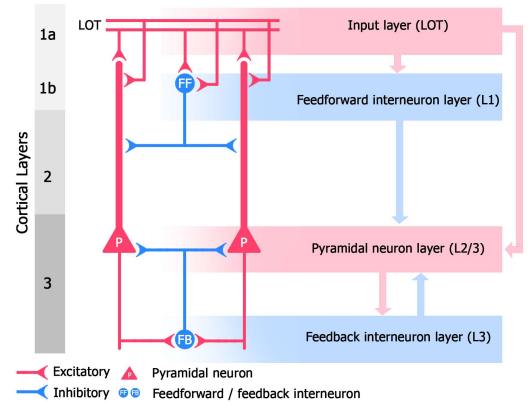


Figure 1. The SNN model to mimic the olfactory cortex

TABLE I. LIST OF PARAMETERS

Neuron and connection		Configuration	
Layer	Name	Type	Number and connection density
LOT	LOT	Poisson input generator	784
	LOT → FF	Excitatory: $g_e = 0.2 \text{ nS}$	50%
	LOT → PYR	Excitatory: $g_e = 0 \sim 0.2 \text{ nS}$	100%
L1	FF	Regular spiking neuron <sup>a</sup>	1024
	FF → PYR	Inhibitory: $g_i = 0.6 \text{ nS}$	29%
L2/3	PYR	Regular spiking neuron <sup>b</sup>	1024
	PYR → FB	Excitatory: $g_e = 15 \text{ nS}$	18%
L3	FB	Fast-spiking neuron <sup>a</sup>	1024
	FB → PYR	Inhibitory: $g_i = 1.2 \text{ nS}$	35%

a. In pyramidal neurons,  $\tau_e = 10 \text{ ms}$  and  $\tau_i = 20 \text{ ms}$

b. In GABAergic interneurons,  $\tau_e = 5 \text{ ms}$

During unsupervised learning, the synaptic weights of the neurons at the pyramidal layer receiving neural signals from the input layer were plastic and can be updated through STDP, while the other synaptic weights were fixed. In addition, threshold potentials of the pyramidal neurons were modulated

according to a homeostasis-like rule to balance the firing rates of all pyramidal neurons during the supervised training [3]. Configuration parameters of neurons and synapses were determined according to the measurement in anesthetized rats [10] and adjusted within in the biologically plausible range as listed in Tab.1.

### C. Temporal Encoding of Handwritten Digit Images

The input layer resembled LOT projections carrying odorant information encoded by the mitral and tufted cells in the olfactory bulb. The mitral and tufted cells encode odor information with a temporal spike coding scheme, and time-synchronized to the inhalation onset of a respiratory cycle [11]. Behavioral animal experiments and optogenetic neural interventions have demonstrated that odor types can be differentiated through analyzing the temporal spike sequences. Odor type is largely contained in the temporal spike sequence of the first 100 ms after inhalation [11], [12].

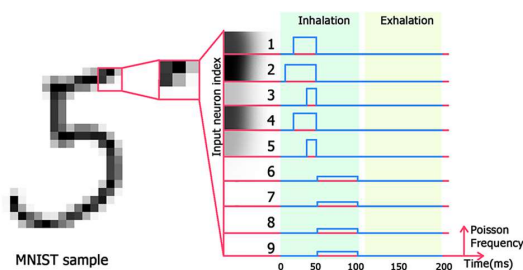


Figure 2. The encoding process for the temporal code

In this study, MNIST hand-written images were used to mimic the semi-2D encoding of the glomeruli at the olfactory bulb. Since the mitral and tuft cells encode the odor type with a temporal code scheme, the pixel intensities of the MNIST images were then converted to temporal spike sequences to mimic the outputs of the olfactory bulb. The time-encoded spike sequence was then projected to the SNN cortical layers through the LOT input layer. The MNIST handwritten digit dataset contains 60,000 labeled images for training and 10,000 additional labeled images for evaluation. All the images are handwritten digits of 0 to 9 collected from a large population and the images were formatted to have an image dimension of  $28 \times 28$  pixels [6]. This image dimension is somewhat comparable to the glomeruli structure in the olfactory bulb.

Parameters for temporal encoding were obtained from reported spike patterns in the mammalian olfactory bulb [11]. A typical respiratory cycle for a rodent is in the order of 200 ms (the first 100 ms for inhalation and the latter 100 ms for exhalation), and it has been determined that odor information is largely represented by the spiking activities at the olfactory bulb during the first 100 ms inhalation period. Therefore, the intensity of an MNIST image pixel was translated to a start time for a bursting spike sequence. More specifically, during the first 50 ms, mimicking the onset of the inhalation, the input neurons produced a 150 Hz burst of spikes with a start latency between 0 and 50 ms, which was linearly extrapolated to a pixel intensity between 1 and 255. In this manner, a dark pixel fired much earlier than that of a light pixel. During the time period between 50 to 100 ms, pixels with zero intensity fired with a 5 Hz Poisson spike sequence to reduce synaptic weights that have no contributions to the classification. During the

exhalation period between 100 and 200 ms, all the neurons stopped firing to mimic no information is encoded during this period.

### D. Training and Testing

A training and testing scheme for the SNN model was employed [3] in which the SNN model was trained in an unsupervised manner using the 60,000 MNIST training samples with no labeling. After the SNN had learned all the 60,000 images, the synaptic weights of the pyramidal neurons in the network were fixed and the hemostatic threshold potentials of the pyramidal neurons were also reset to their initial values. At this stage, the pyramidal neurons have learned the handwritten digits in their receptive fields, but an additional step was required to assign each of the pyramidal neurons to one of the 10 classes (digit 0 to 9). A series of training samples were again inputted to the SNN to associate the pyramidal neurons with their pre-classified labels. The pyramidal neuron stimulated by the training image with the highest firing response was associated with the pre-classified label of the training image. Once all the neuron has been associated, the training was finished. The performance of the trained SNN was evaluated by feeding the remaining 10,000 MNIST testing samples to the network to determine its discrimination accuracy. The discrimination accuracy was determined by comparing the label of the highest firing pyramidal neuron to the pre-classified label of the testing image. If a particular testing image did not elicit any pyramidal neuron firing, the testing image was fed again to the SNN with a 20% increase in the burst frequency.

## III. RESULTS

The synaptic weights ( $w$ ) of a pyramidal neuron trained through the unsupervised learning can be visualized by arranging the 784 synaptic weights into a  $28 \times 28$  image. Fig. 3 shows 100 weight images, randomly selected among all the 1024 pyramidal neurons in the input layer, forming a  $10 \times 10$  image mosaic. Distinctive digits can be recognized on all the weight images, indicating that the digit patterns have been learned through unsupervised learning for the SNN. These learned digits can be considered as the receptive fields of the pyramidal neurons, and when an image best matched to one of the receptive fields, the pyramidal neuron then fired first and all the other pyramidal neurons were suppressed by the inhibitory interneurons. This behavior may be similar to odor decoding in the olfactory cortex in which odor-specified spatiotemporal codes were encoded by the olfactory bulb [11].

Fig. 4 (a) shows the corresponding confusion matrix for the SNN. Using the 1000 MNIST testing images, the SNN model achieved an average discrimination accuracy of 60.23% of all the 10-digits. The overall discrimination accuracy was not high due to large variations in discrimination accuracies among the digits. The SNN network had the highest accuracy for digit '1', achieving an accuracy of 91.8%, followed by  $\sim 77\%$  for digits '0' and '9', but remarkably low accuracies for the digits '4' and '5' of  $\sim 26\%$ . The remaining digits had an accuracy of  $\sim 60\%$ .

Since most olfactory discrimination experiments were performed under a binary odor discrimination scheme, the results can be further analyzed by paring the 10 digits to binary discriminations. The accuracy of the binary discriminations

was computed pair by pair and shown in Fig. 4 (b). In binary discrimination, the baseline accuracy is 50% for random choices. In this analysis, the average accuracy of all digit pairs is 78.92% and the highest accuracy was obtained for the ‘0’ and ‘1’ pair, achieving an accuracy of 92.70%. The lowest performing pair was the ‘4’ and ‘9’, with an accuracy of only 63.90%.

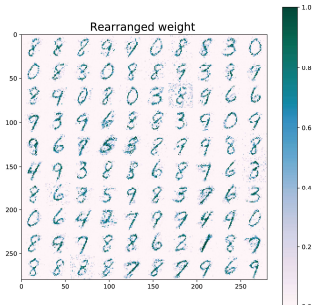


Figure 3. Synaptic weights between the input neurons and pyramidal neurons (100 examples randomly chosen from 1024 neurons). Colorbar indicates maximum (dark green) and minimum (white) synaptic weights.

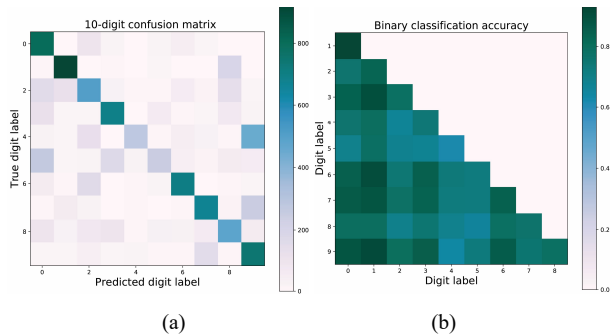


Figure 4. (a) Confusion matrix for 10-digit discrimination (b) Binary discrimination accuracies for the digit pairs.

#### IV. DISCUSSION

In this study, MNIST handwritten images were classified using an SNN mimicking the olfactory cortex. There were some challenges for the SNN to achieve high overall discrimination accuracy, possibly due to some of the fundamental differences between odor stimuli and MNIST images. For odor stimuli, the neural information propagating from olfactory receptor neurons to the piriform cortex is relatively stable, and this information stability may be one of the reasons why the olfactory system is relatively robust against concentration variations and background interference [1]. In contrast, MNIST images suffered from translational and rotational shifts of information, making the discrimination much more challenging. In addition, some of the handwriting digits are very similar and have large overlapping regions, such as ‘3’, ‘5’, ‘8’, and these similarities contributes to much lower discrimination accuracies for these digits. This situation can be considered similar to using odor mixtures, rather than using pure compounds, for animal odor discrimination tasks. To this end, our discrimination performance was actually well-matched to that of animal behavioral odor discrimination tasks using odor mixtures [13]. When rats were trained to do binary odor discrimination task for water rewards, the discrimination accuracy can be as high as 90-95% for pure odors, but the accuracy dropped to 60-65% when odor mixture was used with concentration ratios of 32/68 and 68/32 [2], [13].

From this study, several differences between temporal coding and rate code were observed. The temporal code is more time-efficient and can yield much faster response in discrimination tasks. In this study, the entire encoding and resting time for each image was 200 ms, which is significantly shorter than 500 ms typically used in rate-based networks [3]. With tweaking, it is possible to further reduce the epoch under 100 ms, as in rapid sniffing of rodents. In addition, there are also noticeable differences in the receptive fields using the two coding schemes. Due to the competitive nature of the feedforward and the lateral inhibitions, synapses between the input neurons and the pyramidal neurons were more likely to update the synaptic weights with the early incoming spikes, representing higher intensity pixels. As a result, receptive fields generated using temporal codes tended to form thin strokes. In contrast, receptive fields generated by rate coding tends to have much thicker strokes [3]. These thicker strokes may contribute to higher tolerance in identifying shifted and rotated handwritten digits. On the other hand, in real olfactory systems, the relatively sparse connections of the receptive fields learned through temporal codes may possibly provide a more robust odor discrimination due to a more stable odor representation between the pyramidal neurons and the olfactory receptor neurons.

#### REFERENCES

- [1] J. M. Bekkers and N. Suzuki, “Neurons and circuits for odor processing in the piriform cortex,” *Trends Neurosci.*, vol. 36, no. 7, pp. 429–438, Jul. 2013.
- [2] N. Uchida, C. Poo, and R. Haddad, “Coding and Transformations in the Olfactory System,” *Annu. Rev. Neurosci.*, vol. 37, no. 1, pp. 363–385, Jul. 2014.
- [3] P. U. Diehl and M. Cook, “Unsupervised learning of digit recognition using spike-timing-dependent plasticity,” *Front. Comput. Neurosci.*, vol. 9, no. August, pp. 1–9, 2015.
- [4] B. A. Kaplan and A. Lansner, “A spiking neural network model of self-organized pattern recognition in the early mammalian olfactory system,” *Front. Neural Circuits*, vol. 8, p. 5, Feb. 2014.
- [5] L. de Almeida, M. Idiart, and C. Linster, “A model of cholinergic modulation in olfactory bulb and piriform cortex,” *J. Neurophysiol.*, vol. 109, no. 5, pp. 1360–1377, Mar. 2013.
- [6] Y. Lecun, L. Bottou, Y. Bengio, and P. Haffner, “Gradient-based learning applied to document recognition,” *Proc. IEEE*, vol. 86, no. 11, pp. 2278–2324, 1998.
- [7] E. M. Izhikevich, “Simple model of spiking neurons,” *IEEE Trans. Neural Networks*, vol. 14, no. 6, pp. 1569–1572, Nov. 2003.
- [8] D. J. Saunders, H. T. Siegelmann, R. Kozma, and M. Ruzinkó, “STDP Learning of Image Patches with Convolutional Spiking Neural Networks,” 2018.
- [9] C. C. A. Stokes and J. S. Isaacson, “From Dendrite to Soma: Dynamic Routing of Inhibition by Complementary Interneuron Microcircuits in Olfactory Cortex,” *Neuron*, vol. 67, no. 3, pp. 452–465, 2010.
- [10] C. Poo and J. S. Isaacson, “Odor Representations in Olfactory Cortex: ‘Sparse’ Coding, Global Inhibition, and Oscillations,” *Neuron*, vol. 62, no. 6, pp. 850–861, 2009.
- [11] K. M. Cury and N. Uchida, “Robust Odor Coding via Inhalation-Coupled Transient Activity in the Mammalian Olfactory Bulb,” *Neuron*, vol. 68, no. 3, pp. 570–585, 2010.
- [12] C. D. Wilson, G. O. Serrano, A. A. Koulakov, and D. Rinberg, “A primacy code for odor identity,” *Nat. Commun.*, vol. 8, no. 1, 2017.
- [13] K. Miura, Z. F. Mainen, and N. Uchida, “Odor Representations in Olfactory Cortex: Distributed Rate Coding and Decorrelated Population Activity,” *Neuron*, vol. 74, no. 6, pp. 1087–1098, 2012.